

CHARACTERIZATION OF DYSPHAGIA ONSET
IN A MOUSE MODEL OF
AMYOTROPHIC LATERAL SCLEROSIS (ALS)

A Thesis
presented to
the Faculty of the Graduate School
at the University of Missouri

In Partial Fulfillment
of the Requirements for the Degree
Master of Health Science

by
KAITLIN ALEXANDRA FLYNN
Dr. Teresa E. Lever, Thesis Supervisor

MAY 2017

The undersigned, appointed by the dean of the Graduate School, have examined

the thesis entitled

CHARACTERIZATION OF DYSPHAGIA ONSET IN A MOUSE MODEL OF

AMYOTROPHIC LATERAL SCLEROSIS (ALS)

presented by Kaitlin Alexandra Flynn,

a candidate for the degree of Master of Health Science,

and hereby certify that, in their opinion, it is worthy of acceptance.

Teresa E. Lever, Ph.D.

Mili Kuruvilla-Dugdale, Ph.D.

Emily Leary, Ph.D

ACKNOWLEDGEMENTS

First, I would like to thank my thesis committee chair and mentor, Dr. Teresa Lever, without whom this project would not have been possible. Dr. Lever was a consistent source of guidance, helping me to develop a unique and well-rounded research project. I extend my deepest gratitude for her support throughout this process. She taught me to think critically about others' research and my own, and to always search for a way to improve patient care. Dr. Lever's superior supervision and instruction allowed for the success of this project. Beyond her academic support, Dr. Lever has always shown an interest in her students' personal well-being and happiness. I will always be grateful for the wisdom and friendship Dr. Lever has shared with me.

I would also like to extend a warm thanks to my committee members, Dr. Mili Kuruvilla-Dugdale, and Dr. Emily Leary. Your suggestions and support have been invaluable and have majorly contributed to the development and success of this project. I am forever grateful for your guidance.

My utmost appreciation is to the diligent members of my research team (Victoria Caywood, Brayton Ballenger, Elly Andel) for their hard work and dedication to analyzing hundreds of VFSS videos. Their assistance with data collection was essential to the completion of this project. I would like to extend a heartfelt thanks to Kate Osman for her unwavering mentorship, assistance in the development and completion of this project, and exceptional mouse colony

management. Finally, I would like to thank all of the members of the Lever Lab for creating such a positive work environment over the past few years.

TABLE OF CONTENTS

ACKNOWLEDGMENTS	ii
LIST OF ILLUSTRATIONS	v
ABSTRACT	vi
CHAPTER I: BACKGROUND & INTRODUCTION	1
RESEARCH QUESTIONS AND HYPOTHESES	11
CHAPTER II: METHODS	13
ANIMALS	13
VFSS TESTING TIME POINTS	14
DISEASE ENDPOINT CRITERIA	14
BEHAVIORAL CONDITIONING FOR VFSS TESTING	16
VFSS TESTING PROCEDURE	17
VIDEO ANALYSIS	19
STATISTICAL ANALYSIS	19
CHAPTER III: RESULTS	21
CHAPTER IV: DISCUSSION	32
LIMITATIONS	36
FUTURE DIRECTIONS	38
REFERENCES	40

LIST OF ILLUSTRATIONS

Figure 1. <i>LCN-SOD1</i> MICE DISPLAY DYSPHAGIA AT DISEASE END-STAGE ..	8
Figure 2. VFSS POSITIONING.....	18
Figure 3. LICK RATE DEFICIT EMERGES AFTER 6 MONTHS OF AGE IN <i>LCN-SOD1</i> MICE.....	24
Figure 4. SWALLOW RATE DEFICIT EMERGES AFTER 6 MONTHS OF AGE IN <i>LCN-SOD1</i> MICE.....	25
Figure 5. INTER-SWALLOW INTERVAL DEFICIT EMERGES AFTER 6 MONTHS OF AGE IN <i>LCN-SOD1</i> MICE	26
Figure 6. RADIATION TOXICITY.....	28
Figure 7. DYSPHAGIA SEVERITY DIFFERENCES AT END-STAGE BETWEEN PHENOTYPES.....	31
Table 1. VFSS METRICS	9
Table 2. EXPOSURE TIME POINTS, NUMBER OF EXPOSURES, AND SAMPLE SIZES FOR SINGLE AND SERIAL X-RAY EXPOSURE GROUPS ...	14
Table 3. GROUP SAMPLE SIZES FOR EACH MONTH FOR MICE UNDERGOING SERIAL X-RAY EXPOSURE	22
Table 4. MEAN DIFFERENCE, STANDARD ERROR DIFFERENCE, AND P VALUE FOR VFSS METRICS FOR COMPARISON OF <i>LCN-SOD1</i> (n=13) AND CONTROL MICE (n=11) AT DISEASE END-STAGE IN SERIAL X-RAY EXPOSURE GROUP	23
Table 5. MEAN DIFFERENCE BETWEEN SERIAL (n=24) AND SINGLE X-RAY (n=30) GROUPS AT DISEASE END-STAGE WITH CORRESPONDING STANDARD ERROR OF THE DIFFERENCE AND P-VALUES.....	28
Table 6. MEAN DIFFERENCE, STANDARD ERROR DIFFERENCE, AND P VALUE FOR VFSS METRICS AT DISEASE END-STAGE FOR COMPARISON OF HINDLIMB (n=11) AND FORELIMB + HINDLIMB PARALYSIS (n= 14).....	29

ABSTRACT

The primary goal of this study was to characterize dysphagia onset and progression in the low copy number *SOD1-G93A (LCN-SOD1)* mouse model of ALS. A secondary goal was to determine the effect of serial radiation exposure throughout the lifespan on dysphagia severity. To accomplish this goal, we used our lab's established Videofluoroscopic Swallow Study (VFSS) assay to objectively assess swallow function in 54 mice, divided into serial versus single radiation exposure groups. The serial X-ray exposure group (n=24; 13 *LCN-SOD1*, 11 non-transgenic control) underwent VFSS testing once a month, starting at 2 months of age until disease end-stage. The single X-ray exposure group (n=30; 15 *LCN-SOD1*, 15 non-transgenic control) underwent VFSS testing only once at disease end-stage. VFSS videos from both groups were analyzed to quantify 8 swallow metrics. Results showed that all swallow metrics were similar within and between genotypes from 2 to 6 months of age, which coincided with the pre-clinical disease stage in *LCN-SOD1* mice. At disease end-stage, *LCN-SOD1* mice had significantly altered swallow function for 5 of the 8 VFSS metrics under investigation, compared to age-matched controls. Between disease onset and end-stage, *LCN-SOD1* mice demonstrated highly variable disease phenotypes and survival durations, which rendered it impossible to characterize the onset and rate of dysphagia progression with the small sample size. However, two main findings emerged from this study. First, dysphagia onset in *LCN-SOD1* mice did not occur until after 6 months of age. This finding suggests that treatments for dysphagia in this mouse model of ALS

should begin after 6 months of age (i.e., after clinical disease onset) for optimal translational potential to humans with ALS. Our second novel finding was that dysphagia severity at disease end-stage was similar for single versus serial radiation exposure in *LCN-SOD1* mice, which provides evidence that our lab can continue to perform longitudinal VFSS studies in this small animal without confounding outcomes relative to dysphagia. However, the majority of mice developed evidence of surface-level radiation toxicity (fur depigmentation and dry eyes) as the number of x-ray exposures increased, even though it did not affect swallow function. Therefore, we are taking proactive measures to reduce radiation exposure during VFSS and thereby prevent skin and eye morbidities for future longitudinal dysphagia investigations.

CHAPTER I: BACKGROUND

Introduction

Amyotrophic lateral sclerosis (ALS) is a devastating neuromuscular disease that has no cure and is 100% fatal, with the majority of patients dying within 2-5 years after diagnosis (Bruijn, Miller, & Cleveland, 2004; Cleveland & Rothstein, 2001; Gwinn et al., 2007; Kunst, 2004; Yoshida, Mulder, Kurland, Chu, & Okazaki, 1986). It is estimated to affect 450,000 people worldwide at any given time (Institute, 2015) and is responsible for 2 deaths per 100,000 people each year (Institute, 2015; Orsini et al., 2015; Ticozzi et al., 2011). ALS typically develops after the age of 50 (Orsini et al., 2015; Ticozzi et al., 2011; Yoshida et al., 1986); therefore, it is considered a disease of aging. As such, these epidemiological estimates are expected to dramatically increase given the growing aging population worldwide. While no apparent racial, ethnic, or socioeconomic boundaries have been identified (A. Association, 2015; Wijesekera & Leigh, 2009), there is a slight male predominance (Nelson, 1995; Preston & Shapiro, 2005; Yoshida et al., 1986). In the United States alone, approximately 30,000 people are currently living with ALS, with 5,600 new cases estimated each year – that's 15 new cases a day (A. Association, 2016). Despite being a rare disease, ALS creates a heavy societal burden, costing American taxpayers \$350-450 million per year (M. D. Association, 2015). Mutations in at least 15 different genes have been linked to ALS, including *superoxide dismutase 1 (SOD1)* (Chen, Sayana, Zhang, & Le, 2013; Rosen, 1993; Rosen et al., 1993), which is the focus of this thesis proposal.

The pathological hallmark of ALS is rapid degeneration and **death of motor neurons (MNs)**, specifically upper motor neurons (UMNs) that extend from the cerebral cortex to the brainstem & spinal cord, and lower motor neurons (LMNs) that extend from the brainstem & spinal cord out to the muscles (Brooks, Miller, Swash, Munsat, & Diseases, 2000; Bruijn et al., 2004; Gonzalez de Aguilar et al., 2007; Mitchell & Borasio, 2007; Ravits et al., 2013; Turner et al., 2013). The clinical hallmark is progressive weakness that leads to atrophy (i.e., shrinking, wasting away) and subsequent debilitating paralysis of voluntary (skeletal) muscles of the limbs (arms and legs), bulbar (head and neck) region, & respiration (Ravits et al., 2013). In approximately 30% of ALS cases, the initial clinical symptoms involve the muscles of speech and swallowing; this form is called **bulbar-onset ALS** (Belsh, 1996; Christensen, Hojer-Pedersen, & Jensen, 1990; Hillel & Miller, 1989; Mitsumoto et al., 2003). Approximately 70% of cases have **spinal-onset ALS**, in which muscles of the arms, legs (Kiernan et al., 2011; Wijesekera & Leigh, 2009) or breathing (Kiernan et al., 2011; Orsini et al., 2015; Ravits et al., 2013) are affected first. Limb impairment typically starts in a single arm or leg and spreads to the other limbs (Orsini et al., 2015; Ravits et al., 2013), progressing to wheelchair dependency and ultimately bed-bound status (Institute, 2015). Progressive respiratory deterioration typically results in ventilator dependency (Orsini et al., 2015). Spinal-onset ALS inevitably evolves to affect the bulbar muscles as well. Thus, at some point in the disease process, **nearly all individuals with ALS develop bulbar dysfunction that culminates in the inability to speak or swallow** (Hillel & Miller, 1987; Leder, Novella, & Patwa, 2004; Oliver, 1996; Rio et

al., 2010; Wright & Jordan, 1997). However, **swallowing impairment (dysphagia)** in particular is considered one of the most serious clinical signs because it causes malnutrition and aspiration pneumonia (Ertekin et al., 2000; Hadjikoutis & Wiles, 2001; Higo, Tayama, Watanabe, & Nitou, 2002; Hillel & Miller, 1987; Kawai et al., 2003; Tayama, 1995), both of which are independent risk factors for mortality in ALS (Kuhnlein et al., 2008; Shigemitsu & Afshar, 2007). Moreover, aspiration pneumonia (as a consequence of dysphagia) is directly associated with respiratory failure, which is the leading cause of death in ALS (Corcia et al., 2008; Sejvar, Holman, Bresee, Kochanek, & Schonberger, 2005; Spataro, Lo Re, Piccoli, Piccoli, & La Bella, 2010).

Despite the substantial negative outcomes associated with dysphagia in ALS, research in this area is surprisingly very limited. What we do know is that swallowing deficits in ALS are primarily attributed to **tongue weakness** as a result of progressive degeneration and death of motor neurons in the **hypoglossal nucleus (HN)** in the brainstem, the axons of which directly innervate the tongue via the **hypoglossal nerve** (DePaul, Abbs, Caligiuri, Gracco, & Brooks, 1988; DePaul & Brooks, 1993; Dworkin, 1980; Weikamp, Schelhaas, Hendriks, de Swart, & Geurts, 2012). Tongue weakness is also common in spinal-onset ALS patients without perceptible speech or swallowing deficits (DePaul et al., 1988). This finding suggests HN degeneration occurs early in ALS, regardless of disease onset phenotype (bulbar or spinal) (Weikamp et al., 2012). Further, **impaired tongue strength was recently identified as an independent prognostic indicator of**

shorter survival in ALS patients (Weikamp et al., 2012). As the disease progresses, weakness typically spreads to other muscles involved in swallowing, to include the jaw, lips, pharynx, and larynx (Hillel & Miller, 1989).

Only one study has attempted to characterize dysphagia in ALS using videofluoroscopy, the gold standard dysphagia diagnostic test. This test is commonly referred to as a **videofluoroscopic swallow study (VFSS)**. VFSS is a radiographic (X-ray) procedure that allows visualization of swallowing in real time, as well as video recording of the procedure for subsequent frame-by-frame analysis to quantify swallow function. Using VFSS, Higo et al. (Ryuzabaro, Niro, & Takaharu, 2004) found that dysphagia in ALS is characterized by three main impairments: delayed bolus transfer from the oral cavity to the pharynx, reduced pharyngeal constriction, and reduced elevation of the hyoid and larynx. Thus, additional videofluoroscopic investigations are essential to better characterize the onset and progression of dysphagia in ALS, which we propose is essential for early detection of dysphagia as well as determining the effectiveness of treatment interventions.

There are currently no treatments available to significantly improve dysphagia in people with ALS. The pervasive bulbar muscle weakness in ALS suggests an essential role for therapeutic exercise to improve swallowing function (Plowman, 2015). However, this topic remains highly controversial because available data are insufficient to determine whether exercise is beneficial or harmful for this patient population (Dal Bello-Haas & Florence, 2013; Plowman,

2015). As a result, therapeutic exercise for ALS patients is discouraged by health care providers, due to the fear of overburdening diseased muscles and accelerating disease progression, further compromising the quality and duration of life (Dal Bello-Haas & Florence, 2013; Logemann, 2006). Riluzole, the only Food and Drug Administration-approved pharmacologic intervention for ALS, has been shown to extend median survival by only 2-3 months for most ALS patients (Brooks & Sanjak, 2004; Lacomblez et al., 1996; Orsini et al., 2015). However, this anti-glutamatergic medication has no effect on muscle weakness and does not improve functional outcomes, including those pertaining to swallowing (Miller, Mitchell, Lyon, & Moore, 2007; Miller, Mitchell, & Moore, 2012). Moreover, questions persist about its clinical utility because of high cost (up to \$12,000 per year) and modest efficacy (Miller et al., 2007; Miller et al., 2012). ALS patients are in dire need of more effective and less expensive treatments to positively improve swallow function to increase the quality and duration of life. We propose that mouse models of ALS may play an important role in understanding dysphagia in ALS as well as finding effective treatments to improve swallow function.

The most widely studied mouse model of ALS is the high copy expressing *SOD1-G93A* mouse, henceforth referred to as *HCN-SOD1*. This model expresses ~25 copies of the human *SOD1* gene which carries a G93A mutation (i.e., glycine is substituted for alanine a position 93) (Gurney et al., 1994; *Neurobiology Research and the Laboratory Mouse: A Jackson Laboratory Resource Manual*, 2008; Pfohl, Halicek, & Mitchell, 2015). *HCN-SOD1* mice develop progressive

paralysis of the hindlimbs approximately 3-4 months of age and die approximately 5 months of age. Our preliminary work with this model revealed a tongue motility deficit (i.e., reduced lick rate) at 21 days of age (i.e., at weaning) that progressively worsens as the disease advances (Daghlas et al., 2015). This was quantified using a lick rate assay established in our lab that entails video recording mice while drinking water after an overnight (16 hour) fluid restriction, followed by frame-by-frame video analysis to count each lick cycle, regardless of whether or not the tongue contacted the spout (Lever et al., 2009; Lever et al., 2010). Other labs have used an automated lick rate measuring device that relies on tongue contact (i.e., lickometer). However, a tongue motility deficit was not detected in *HCN-SOD1* mice using this device until 110 days of age (Smittkamp, Brown, & Stanford, 2008). This finding highlights the increased sensitivity of our manual analysis method over automated lickometers.

The developmental tongue motility deficit in *HCN-SOD1* mice renders this model unsuitable for investigations of dysphagia in ALS, which is an adult-onset disease (Daghlas et al., 2015). For this reason, we have turned our efforts to low copy number *SOD1* mice (*LCN-SOD1*) with only 7-10 copies of the *SOD1-G93A* mutation (Acevedo-Arozena et al., 2011; Dal Canto & Gurney, 1997; Gurney, 1997; Jaarsma, Teuling, Haasdijk, De Zeeuw, & Hoogenraad, 2008). Compared to *HCN-SOD1* mice, *LCN-SOD1* mice have a delayed disease onset (occurs approximately 6 months of age) and extended survival (7-9 months of age), making this model ideal for testing new therapeutic approaches initiated *after* clinical

disease onset for improved translational potential to human ALS (Acevedo-Arozena et al., 2011; Dal Canto & Gurney, 1997). Moreover, unlike the stereotypical hindlimb paralysis of *HCN-SOD1* mice, *LCN-SOD1* mice display a highly variable phenotype relative to limb involvement, which has not yet been well-characterized but appears to more closely resemble the phenotypic variability in human ALS (Acevedo-Arozena et al., 2011; Dal Canto & Gurney, 1997; M. E. Gurney, 1997; Jaarsma et al., 2008). Bulbar involvement has not previously been investigated in this *LCN-SOD1* animal model, which is the focus of this thesis proposal.

Our preliminary work with *LCN-SOD1* mice revealed this mouse model of ALS indeed develops dysphagia at disease end-stage (Robbins, Allen, & Lever, 2015). Dysphagia was identified in awake, freely-behaving mice using our standard VFSS protocol and custom low-energy fluoroscope that permits visualization of the entire swallowing mechanism of this small mammal, spanning from the tongue tip to the stomach (**Figure 1**) (Lever, Braun, et al., 2015; Lever, Brooks, et al., 2015). Briefly, mice are exposed to approximately 2 minutes of low-dose radiation while drinking a thin liquid contrast agent (iohexol) in a custom test chamber after an overnight (approximately 16 hr.) water restriction to induce thirst. The chamber (15x15x2 inches) was designed to minimize behavioral distractions to promote voluntary drinking in the lateral plane. To minimize radiation exposure, the fluoroscopy beam is activated only when the mouse is drinking from the bowl, and the mouse is video-recorded at 30 frames per second (fps). Our LabScope

emits low-energy scatter that is known to be absorbed at the body surface (i.e., skin and eyes, rather than deep tissues). The LabScope is lacking low-energy filters that would absorb that scatter and it is instead being absorbed by the mouse. After 3-4 long (10-20 second) bouts of drinking, the mouse is returned to the home cage. The entire VFSS procedure takes up to 30 minutes per mouse.

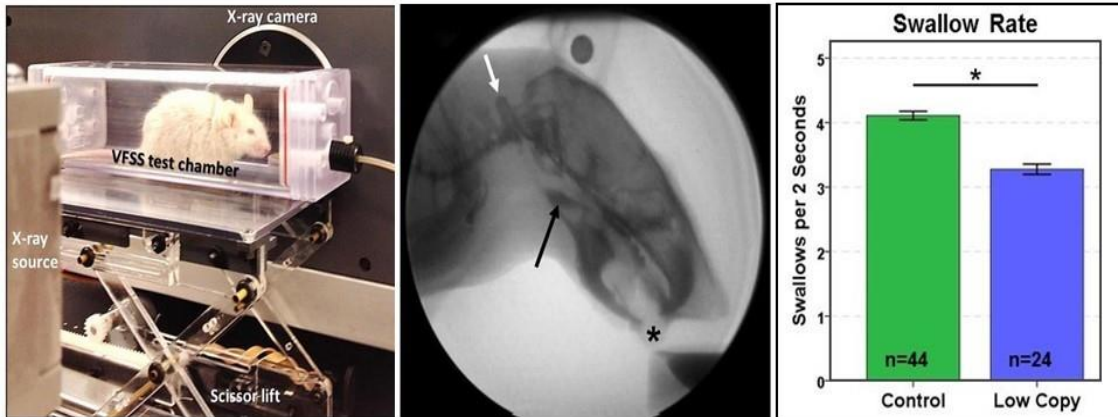


Figure 1. *LCN-SOD1* mice display dysphagia at disease end-stage. Left: Awake, unanesthetized mouse in a custom test chamber undergoing VFSS using our miniature, low energy fluoroscope. **Middle:** Radiographic image of a mouse drinking during VFSS. The swallow trigger point (black arrow; vallecular space) is positioned in the center of the field of view. The tongue (black asterisk) is visible as the mouse drinks liquid contrast (iohexol) from a bowl. With each successive lick, contrast agent accumulates in the pharynx (black arrow) before triggering a swallow. **Right:** At disease end-stage, the swallow rate of *LCN-SOD1* mice is significantly reduced compared to age-matched controls. Asterisk denotes statistical significance ($p < 0.05$).

At a later time, videos are independently analyzed by 2 trained reviewers in blinded fashion to identify five 2-second episodes of uninterrupted drinking at the bowl. From these episodes, several VFSS metrics are manually quantified (**Table 1**), most of which are translatable to humans. Examples include swallow rate and pharyngeal and esophageal transit times. All value discrepancies are subjected to group consensus to resolve reviewer errors. This manual video analysis protocol is time consuming, taking approximately 1.5 hours per mouse.

Table 1. VFSS METRICS (Lever, Braun, et al., 2015; Lever, Brooks, et al., 2015)

Swallow Metric	Description
Swallow Rate*	Swallow rate is defined as the number of swallows that occur during each 2-second interval of uninterrupted drinking. This metric is an indicator of oral transit time as well as pharyngeal swallow delay.
Inter-Swallow-Interval (ISI)*	Inter-swallow interval is defined as the number of video frames between two successive, uninterrupted swallows. The “rest frame”, also known as or “ISI start frame,” is the video frame that directly precedes the frame in which the transfer of the bolus into the pharynx is visible. The ISI end frame is the “rest frame” of the next swallow. The number of frames between the two swallows is then divided by 30 frames per second (fps) to convert to time (ms). This metric is also an indicator of oral transit time and pharyngeal swallow delay.
Pharyngeal Transit Time (PTT)*	Pharyngeal Transit Time is defined as the number of video frames it takes for the bolus to clear the pharynx from the onset of the swallow. The PTT start frame is identical to the ISI start frame. The PTT end frame is defined as the frame at which the bolus has fully passed the 2 nd cervical vertebra. The number of frames between the start and the end frame is then divided by 30 frames per second (fps) and converted to milliseconds (ms).
Esophageal Transit Time (ETT)*	The Esophageal Transit Time start frame is identical to the Pharyngeal Transit Time end frame. The ETT end frame is identified as when the bolus has completely entered the stomach and is no longer visible in the esophagus. The number of frames between the start and end frame is then divided by 30 fps and converted to milliseconds.
Jaw Excursion Rate (Lick Rate)	Jaw excursion rate is quantifiable for lick rate, as the tongue is not always visible during testing. The number of jaw excursion cycles (i.e., open/close cycles) can be used as a substitute for tongue protrusion/retraction cycles. Jaw excursion rate is defined as the number of jaw open/close cycles per second (30 frames). Each cycle begins when the jaw is maximally open and ends when jaw returns to the maximally open position. Each subsequent cycle is counted as an individual jaw excursion cycle.
Lick-swallow-ratio	Lick-swallow Ratio is defined as the number of jaw excursion cycles that occur between two successive, uninterrupted swallows. It is an indicator of oral transit time and pharyngeal swallow delay.
Effective Esophageal Swallows*	Effective Esophageal Swallows is a metric used to identify if a second swallow is necessary to force the preceding swallow into the stomach. To quantify this, uninterrupted swallowing is observed in position two. A successful initial swallow entails that the bolus completely enters the stomach before a subsequent swallow is triggered.
Number of swallows to clear esophagus*	Number of Swallows to Clear the Esophagus is calculated after determination of Effective Esophageal Swallows. If the bolus of one swallow does not clear the esophagus before a second uninterrupted swallow occurs, the reviewer is to count how many swallows occurred before the complete transfer of the first swallow into the stomach (i.e., ETT end frame).
Bolus Area*	Bolus Area is quantified by first capturing three still frame images at the ISI start frame using Pinnacle 14 software. Next, the images are viewed using NIH Image J software. A tracing of the bolus is created and the area inside the tracing is calculated. Each photo’s measurements are calibrated to the radiographic calibration marker visible during VFSS testing. Measurement of all three boluses’ will follow this procedure and will be completed separately by two reviewers. Reviewers will individually average their three recorded measurements. Finally, the two averages will be averaged together to create a final bolus area measurement.

*Signifies swallow metric is translatable to humans

Preliminary results using this protocol showed that end-stage *LCN-SOD1* mice had significantly impaired swallow function compared to age-matched littermate controls. Specifically, *LCN-SOD1* mice had significantly reduced swallow rates, longer inter-swallow intervals, longer pharyngeal and esophageal transit times, reduced lick rates, and smaller bolus areas (Robbins et al., 2015). For this thesis project, we expanded upon our lab's preliminary work by using VFSS to characterize dysphagia onset and progression on a monthly basis across the life-span of *LCN-SOD1* mice. Identification of dysphagia onset is essential to the design of our future therapeutic investigations with *LCN-SOD1* mice, which will determine the optimal timing to initiate various dysphagia treatments. This approach provided essential information about timing of dysphagia onset and the rate of dysphagia progression for comparison with our future therapeutic investigations with this mouse model of ALS.

A caveat of monthly VFSS across the lifespan is the unknown effect of serial, low dose radiation exposure on swallowing function in mice (Lever, Braun, et al., 2015; Lever, Brooks, et al., 2015). Other mouse strains undergoing serial VFSS testing in our lab have developed visible signs of radiation toxicity of the skin (depigmentation of the fur) and eyes (excessive drying) on the side of the body closest to the X-ray source, indicative of surface absorption of low energy X-ray scatter. However, it is unknown if the deeper tissues/structures involved in swallowing are also affected. To address this potential confound, we designed this study to compare the effect of single vs. multiple radiation exposures on

swallowing function in *LCN-SOD1* mice. To do this, we utilized a group of mice that were tested only once at disease end-stage (disease end-stage for each mouse was determined by the criteria explained in the results section of this thesis) for comparison with a different group of mice that were tested monthly, beginning at two months of age until they reached disease endstage. This approach allowed us to determine if serial X-ray exposure altered the timing of dysphagia onset or rate of dysphagia progression.

Research Questions and Hypotheses

Using VFSS testing, we addressed the following research questions and hypotheses.

1. What is the mean age of dysphagia onset in *LCN-SOD1* mice?
 - a. We hypothesized that onset of dysphagia would occur after mice had fully developed (i.e., after two months of age), as opposed to *HCN-SOD1* mice who develop dysphagia at weaning (Daghlis, 2015).
2. How does the dysphagia profile and severity change with ALS disease progression?
 - a. We hypothesized that fewer outcome measures would be affected at dysphagia onset compared to disease end-stage, and dysphagia severity would be less at onset vs. endstage. Because lick rate is affected at weaning age in *HCN-SOD1* mice (Daghlis, 2015), we

expected lick rate would be the first indication of dysphagia in *LCN-SOD1* mice.

3. Does monthly radiation exposure over the lifespan (beginning at 2 months of age until disease end-stage) impact dysphagia severity?
 - a. Given the low energy X-ray produced by our fluoroscope and the limited (<2 minutes) exposure time per month, we hypothesized that the number of radiation exposure times would not influence dysphagia severity. In other words, endstage mice with a single exposure would have similar dysphagia severity as those with monthly exposures across the lifespan.

CHAPTER II: METHODOLOGY

Animals

A total of 54 *LCN-SOD1* mice from our established colony were included in this study. Offspring were weaned at 21-24 days of age as well as earpunched (for identification purposes) and tailsnipped (for genotyping purposes). Mice were then group housed based on sex (2-4 per cage) in standard vivarium conditions. Free access to food and water was provided, except during behavioral testing time-points as described below. To minimize aggressive behaviors in group housing, mice were provided with enrichment materials (e.g., huts, running wheels, dental treats, nestlet, etc.) that were replenished weekly. Mice were monitored daily by veterinary and research staff to ensure their health throughout this study (with the exception of signs of ALS).

A quantitative PCR (i.e., polymerase chain reaction) method, developed by Alexander et al., was used to determine the genotype of all offspring in this study. This method was also used to ensure that all mice maintained the standard number of copies of the *SOD1* gene (i.e., approximately 8 to 10 copies). Although it is rare, dropped copies can occur during mating. Researchers were blinded to the genotypes of the mice throughout data collection and analysis until the ALS phenotype became visibly apparent.

VFSS Testing Time Points

Fifty-four mice were divided into 2 test cohorts: single versus serial X-ray exposure, as shown in **Table 2**. For single X-ray exposure, a cohort of mice (n=30) had VFSS testing only once at disease end-stage. For serial X-ray exposure, a separate cohort of mice (n=24) underwent VFSS testing once a month, starting at 2 months of age until disease end-stage.

Cohorts	Exposure Time Points	# Exposures	Sample Size
Single X-ray Exposure	Disease end-stage	1	n=30 (15 control, 15 <i>LCN-SOD1</i>)
Serial X-ray Exposure	Monthly (2 months old until disease end-stage)	6-9 (due to variable phenotype progression*)	n=24 (11 controls, 13 <i>LCN-SOD1</i>)
Total number of mice			n= 54

*The highly variable phenotype necessitates the use of endpoint criteria that are independent of limb involvement

Disease Endpoint Criteria

Our lab has identified 3 main phenotypes in *LCN-SOD1* mice: predominant hindlimb paralysis (bilateral), predominant forelimb paralysis (bilateral), and hemiparalysis (paralysis of ipsilateral hindlimb and forelimb) (Robbins et al., 2015). We routinely used three assessments (described below) to identify when each mouse had reached a humane endpoint that corresponds to disease end-stage. Each assessment defines an independent endpoint criterion, and each mouse was

euthanized when at least one endpoint criterion had been met. We have found that mice allowed to live past these criteria are typically found dead in their cage, thereby preventing histological analyses for correlation with clinical outcomes. Testing occurred weekly until limb paresis was apparent, at which time disease progression is accelerated and more often (up to daily) testing was necessary to detect when mice had reached disease end-stage.

i. Righting Reflex Assessment – The humane end-point for virtually all studies of ALS mouse models continues to be loss of the righting reflex, defined as the inability of a mouse to return to sternal position after being placed on its side. While the latency cutoff varies between labs, 10-30 s is most commonly used (Boillee, Vande Velde, & Cleveland, 2006; Hayworth & Gonzalez-Lima, 2009; Milanese et al., 2014; Rao, Campbell, Palaniappan, Kumar, & Nixon, 2016; Stoica et al., 2016; Su, Nandar, Neely, Simmons, & Connor, 2016; Wang et al., 2016). We chose the more conservative righting reflex latency of 10 s for our study, as we have found that longer latencies are associated with fewer spontaneous drinking episodes during VFSS testing, resulting in missing data that compromises statistical analysis. The latency until each mouse rights itself from either side was recorded, and a latency of ≥ 10 s *for either side* for 2 consecutive days served as an independent endpoint criterion.

ii. Body Weight Assessment – Weekly body weight (g) was collected for each mouse using a digital balance. To avoid diurnal variations, weighing was performed at approximately the same time every day. Weight loss of $\geq 30\%$ from

maximum body weight served as an independent endpoint criterion (Jaarsma et al., 2008; Mead et al., 2011).

iii. Fecal Assessment – Fecal assessment was performed weekly to detect mice at risk for fecal impaction of the rectum. Normal mice scatter their feces relatively evenly around the home cage, without evidence of fecal impaction or soiling of the urogenital region. Affected mice leave small piles of feces or visibly less fecal scatter as limb paralysis develops, indicative of reduced ambulation within the cage. At the onset of limb paresis, mice were assessed daily to detect fecal impaction that is readily visible as a fecal plug blocking the rectal opening. The impaction was gently removed with a dampened cloth and daily fecal assessments resumed until impaction returned. The second episode of fecal impaction served as an independent endpoint criterion.

Behavioral Conditioning for VFSS Testing

Mice were behaviorally conditioned (i.e., primed) with the VFSS test solution to familiarize them with the taste and promote sufficient drinking behavior during testing (Lever, Braun, et al., 2015; Lever, Brooks, et al., 2015). Priming occurred twice per week beginning at weaning until mice reached 2 months of age, at which time priming occurred once a week until the end of life. To avoid a possible development of a taste aversion prior to testing, the contrast agent (iohexol) was not used during priming. During priming, food and water were removed from the home cage. A sipper tube bottle containing a chocolate solution was inserted

though an opening in the top of the test chamber, which was then placed in the home cage for approximately 2 hours. This allowed the mice to become familiar with drinking the solution inside of the test chamber. After priming, food and water were returned to the home cage.

VFSS Testing Procedure

Mice underwent VFSS testing at their respective time-points in accordance with the protocol developed in our lab (Lever, Braun, et al., 2015; Lever, Brooks, et al., 2015). Testing occurred after an overnight (approximately 16 hour) water restriction to induce thirst and encourage maximum drinking performance during testing. Mice were given food pellets overnight, however water was not provided. Treats (nuts and seeds) were also provided overnight to induce thirst. The test chamber was placed in the home cage overnight (with one end-cap attached), which permitted mice to become familiar with the test environment. This also allowed the mice to transfer their smell to the test chambers in hopes of reducing stress levels during VFSS testing.

The following morning, the test chambers were rinsed off with water to remove waste and improve transparency to improve visual resolution of the VFSS videos. Mice were gently guided into the test chamber and the second end-cap that contains a drinking bowl was placed on the other end of the chamber. The test chamber was then placed on the fluoroscopy platform and positioned between the X-ray source and camera. The test solution was administered into the bowl via our

custom syringe delivery system. A webcam was positioned above the test chamber to provide real-time viewing of mice throughout the procedure. To limit radiation exposure to <2 minutes per time point, the fluoroscope was manually powered on (using a foot pedal) when the mouse approached the bowl and was turned off when the mouse turned away from the bowl. Video recordings were captured with mice in both the oral-pharyngeal stage of swallowing (Position 1) and the esophageal stage of swallowing (Position 2), as displayed in **Figure 2**.

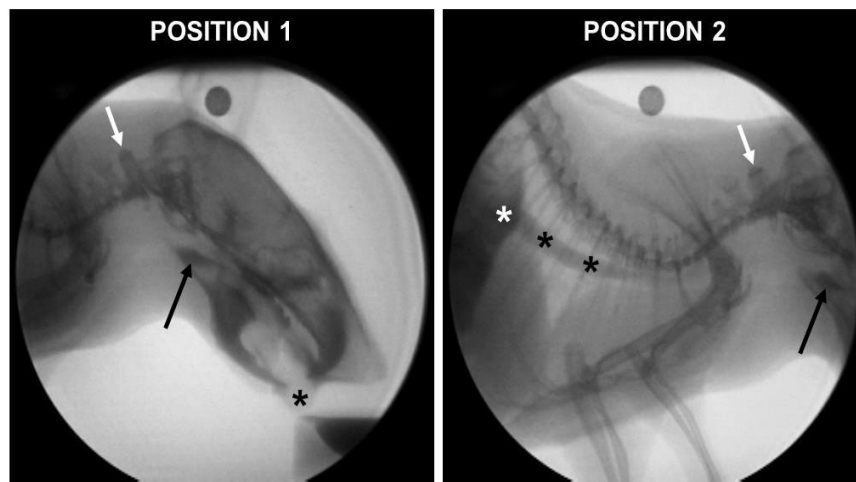


Figure 2. VFSS Positioning in our miniature fluoroscope. The above radiographic images show a mouse during voluntarily drinking. The test chamber is moved via remote-controlled platform to position the mouse within the X-ray beam to capture the oral & pharyngeal (**Position 1**) and esophageal (**Position 2**) stages of swallowing. Position 1: The head and proximal thoracic region are visible in the fluoroscopy field of view (FOV), with the swallow trigger point (black arrow; vallecular space) positioned in the center. The tongue (black asterisk) is visible as the mouse drinks from a bowl. With each successive lick, contrast agent accumulates in the pharynx (black arrow) before triggering a swallow. Position 2: The FOV spans from the swallow trigger point (black arrow) to the stomach (white asterisk). Note the bolus (black asterisks) passing through the distal esophagus. White arrows: 2nd cervical vertebra.

Video Analysis

VFSS videos were independently analyzed by two reviewers using Pinnacle Studio 14 (Pinnacle Systems, Inc.) video editing software. Reviewer 1 identified five 2-second episodes of uninterrupted drinking at the bowl, from which several VFSS metrics were manually quantified. Reviewer 2 was blinded to values determined by reviewer one, with the exception of the start frame for each 2-second episode. All value discrepancies between reviewers were subjected to group consensus to resolve reviewer errors and ensure reliability of data. Videos were analyzed to quantify our standard swallow metrics which are listed and described in **Table 1**.

Statistical Analysis

Summary statistics were calculated for each VFSS swallow metric. Measures of central tendency, including mean, and measures of variability, including standard deviation, were calculated for continuous swallow metrics and frequencies were calculated for categorical swallow metrics. A repeated measures ANOVA for the serially exposed mice was used to compare mean swallow metrics within and between genotypes from two to six months of age. A two-sided independent samples T-test was used to test mean differences in VFSS swallow metrics between the serially and singly VFSS exposed mice at disease end-stage. Secondary analyses were conducted considering group comparisons between the ALS phenotypes. A two-sided independent samples t-test was used to test the mean difference in VFSS swallow metrics at disease end-stage between the ALS

phenotypes. For all analyses, two-sided significance levels were used with alpha set at 0.05. All analyses were completed using SPSS v23 (IBM).

CHAPTER III: RESULTS

Fifty-four mice underwent testings and a total of 207 videos were analyzed for this study. All VFSS swallow metrics were analyzed as planned, with the exception of bolus area. Due to an unexpected calibration error in our VFSS system, data for bolus area was inaccurate and therefore excluded from statistical analysis. This error has been corrected so that bolus area can be included in future investigations in our lab. Results identified which of the swallow metrics were dysfunctional in the *SOD1-LCN* transgenic mice.

To answer Research Question 1 (**What is the mean age of dysphagia onset in *LCN-SOD1* mice?**), a repeated measures ANOVA with post-hoc comparisons for each of the swallow metrics were used to detect when significant differences emerge. We focused on the time span between 2 and 6 months of age because all *LCN-SOD1* mice survived a minimum of 6 months. However, after 6 months of age, *LCN-SOD1* mice demonstrated variable disease progression and survival durations, such that the sample size was markedly reduced each successive month. In addition, age-matched control mice were selectively euthanized to correspond with the disease end-point of affected mice, allowing for collection of tissues and subsequent histological analysis, which is beyond the scope of this thesis project. As a result, it was not possible to characterize the onset and rate of dysphagia progression using statistical analyses. To circumvent this issue of attrition (rapid reduction in number of mice per timepoint), we limited

our repeated measures ANOVA analysis to complete data (i.e., 2 to 6 months of age), as shown in **Table 4**.

Table 3. GROUP SAMPLE SIZES FOR EACH MONTH FOR MICE UNDERGOING SERIAL X-RAY EXPOSURE									
GENOTYPE	AGE (months)								
	2	3	4	5	6	7	8	9	10
Control	11	11	11	11	11	11	10	9	4
<i>LCN-SOD1</i>	13	13	13	13	13	11	8	3	1

Results showed that between 2 and 6 months of age, there were no statistically significant differences within and between genotypes (*LCN-SOD1* and controls) for any of the swallow metrics. Therefore, dysphagia onset emerges after 6 months of age in this mouse model of ALS. Next, we included only the final VFSS timepoint for each mouse at its humane endpoint in the study (referred to as “end-stage” in illustrations) to demonstrate that *LCN-SOD1* mice do develop dysphagia as was shown by a previous thesis project in our lab (Braun, 2015). To do this, we ran independent samples T-tests (two-sided) to compare each VFSS swallow metric between genotypes (*LCN-SOD1* and controls) at only the end-stage timepoint of the serial X-ray exposure group. Results showed that 5 of the 8 swallow metrics (lick rate, swallow rate, inter-swallow interval, effective esophageal swallows, and number of swallows to clear esophagus) were significantly different in *LCN-SOD1* mice at disease end-stage, compared to age-matched controls, as shown in **Table 5**. Representative results are graphically

summarized in **Figures 3-5** for 3 of the 5 impaired swallow metrics to demonstrate a general trend.

Table 4. MEAN DIFFERENCE, STANDARD ERROR DIFFERENCE, AND P VALUE FOR VFSS METRICS FOR COMPARISON OF *LCN-SOD1* (n=13) AND CONTROL MICE (n=11) AT DISEASE END-STAGE IN SERIAL X-RAY EXPOSURE GROUP

Swallow Metrics	Mean Difference	Std. Error Difference	p value
Lick Rate	1.899	.177	<.0001
Swallow Rate	.810	.151	<.0001
Lick-Swallow Ratio	-.503	.426	.241
Inter-Swallow interval	-.235	.049	<.0001
Pharyngeal Transit Time	.002	.004	.651
Esophageal Transit Time	.052	.107	.625
Effective Esophageal Swallows	-.322	.097	.002
Swallows to Clear Esophagus	.574	.146	<.0001

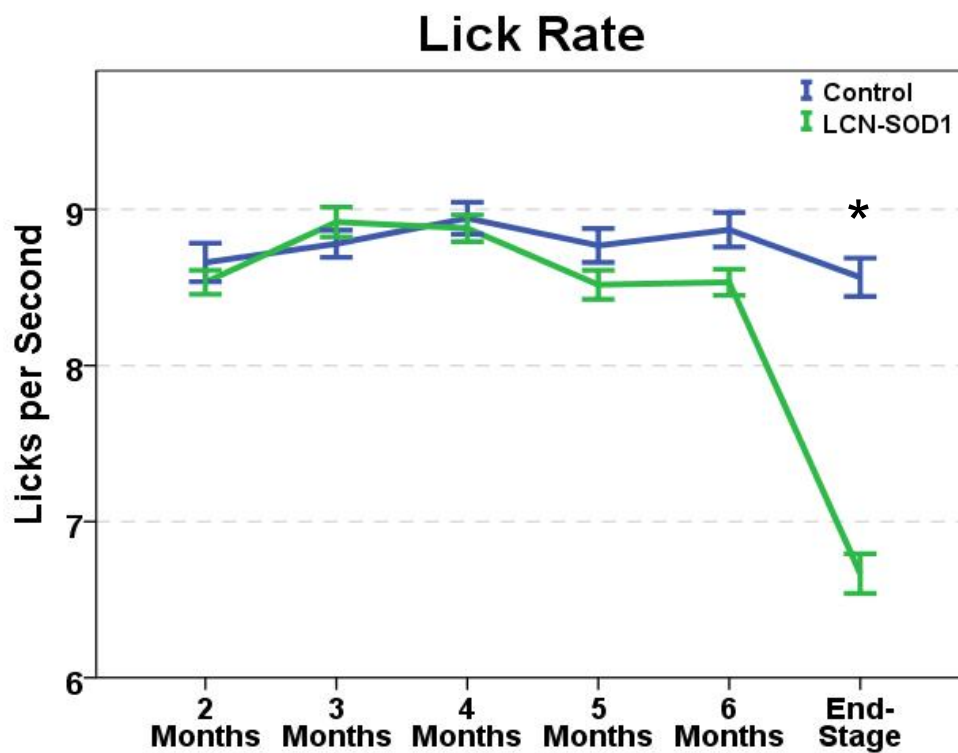


Figure 3. Lick rate deficit emerges after 6 months of age in *LCN-SOD1* mice. Compared to controls, lick rate impairment in *LCN-SOD1* mice does not emerge until after six months of age, during the rapid disease progression stage. Beginning at 5 months of age, the lick rate of *LCN-SOD1* mice begins to slow, compared to age-matched controls. However, this difference does not reach statistical significance until disease end-stage, at least with the small sample size included in this study. Asterisk denotes statistical significance ($p < .05$); error bars = mean \pm 1 standard error of the mean (SEM).

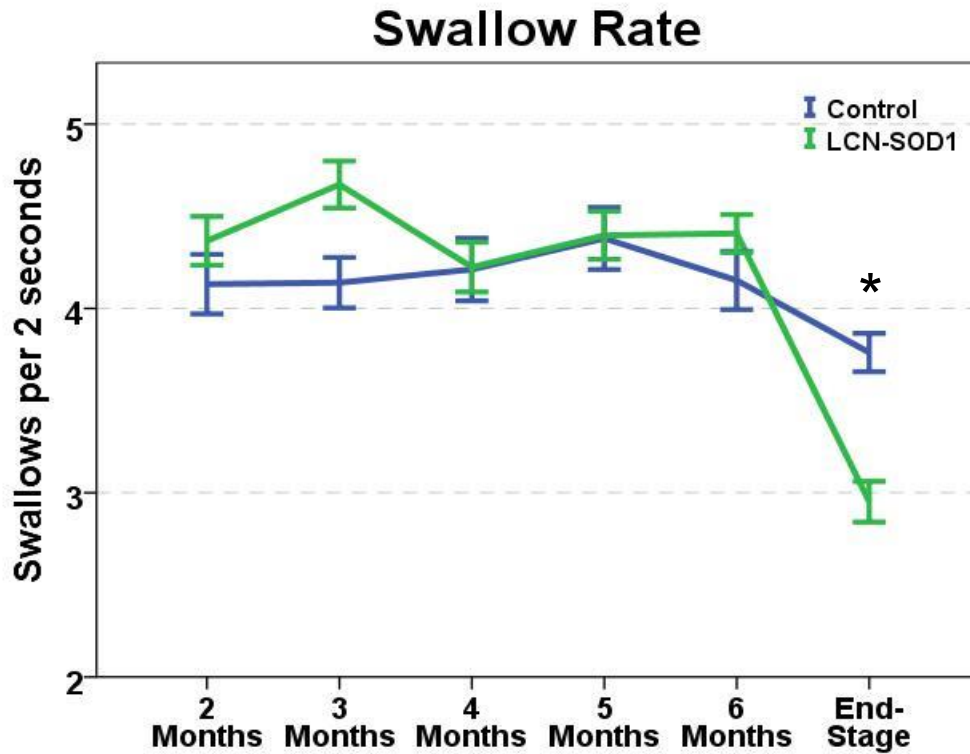


Figure 4. Swallow Rate deficit emerges after 6 months of age in *LCN-SOD1* mice. Compared to controls, swallow rate impairment in *LCN-SOD1* mice does not emerge until after six months of age, during the rapid disease progression stage. Asterisk denotes statistical significance ($p < .05$); error bars = mean \pm 1 standard error of the mean (SEM).

Inter-Swallow Interval

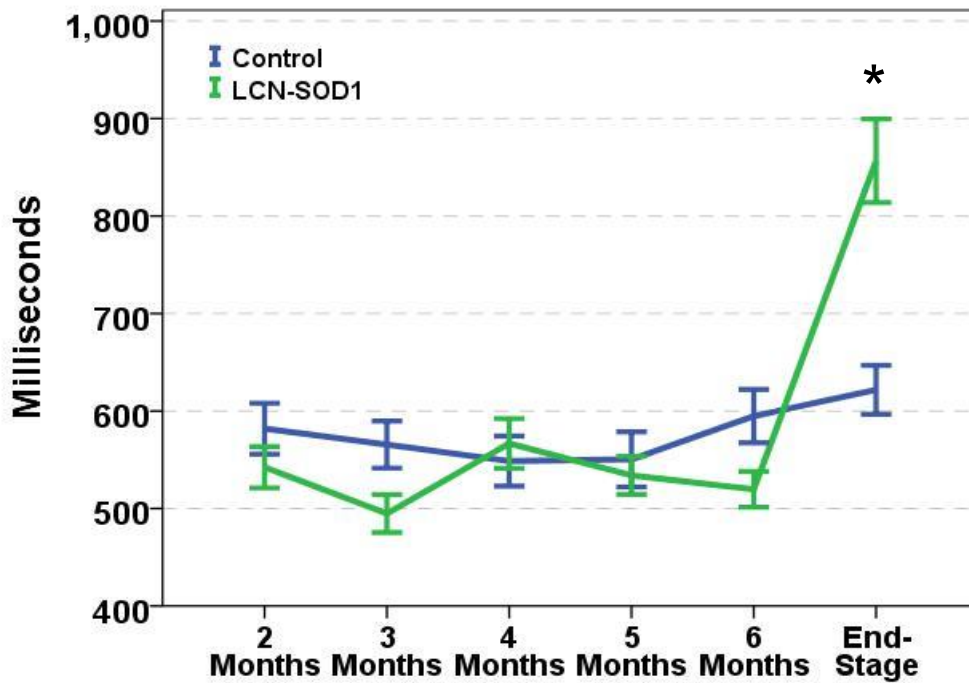


Figure 5. Inter-swallow interval deficit emerges after 6 months of age in *LCN-SOD1* mice. Compared to controls, inter-swallow interval impairment in *LCN-SOD1* mice does not emerge until after six months of age, during the rapid disease progression stage. Asterisk denotes statistical significance ($p < .05$); error bars = mean \pm 1 standard error of the mean (SEM).

To answer Research Question 2 (**How does the dysphagia profile and severity change with disease progression?**), we relied on descriptive observations rather than statistical analyses, due to the marked attrition after 6 months of age. From 2 to 6 months of age, swallow function remained stable in both genotypes (*LCN-SOD1* and controls), as described in the results from research question 1. After 6 months of age, *LCN-SOD1* mice *variably* progressed to disease end-stage. The humane end-point (i.e., the final VFSS test date) was the timepoint at which swallow function was the most severely impaired.

Fifty-four mice underwent VFSS testing, divided into the single versus serial X-ray exposure groups. For the single X-ray exposure group, mice were tested only once upon reaching disease end-stage criteria. For the serial X-ray exposure group, testing was completed as planned from 2 months of age until mice reached disease end-stage. To answer Research Question 3 (**Does monthly radiation exposure from 2 months of age until disease end-stage impact dysphagia severity?**), we used independent samples T-tests (two-sided) to compare each VFSS swallow metric between the serial X-ray exposure group and single X-ray exposure group at disease end-stage. Results showed there was no statistically significant difference between groups for any of the VFSS swallow metrics, as shown in **Table 6**. All mice in the serial X-ray exposure group were tested between 6 and 9 times (i.e., until disease end-stage was reached), spaced at one month intervals.

TABLE 5: MEAN DIFFERENCE BETWEEN SERIAL (n=24) AND SINGLE X-RAY (n=30) GROUPS AT DISEASE END-STAGE WITH CORRESPONDING STANDARD ERROR OF THE DIFFERENCE AND P-VALUES.

Swallow Metrics	Mean Difference	Std. Error Difference	p value
Lick Rate	.030	.191	.874
Swallow Rate	.049	.174	.780
Lick-Swallow Ratio	-.475	.397	.234
Inter-Swallow interval	.014	.073	.844
Pharyngeal Transit Time	.002	.003	.560
Esophageal Transit Time	.142	.098	.151
Effective Esophageal Swallows	-.065	.118	.563
Swallows to Clear Esophagus	.365	.183	.056

Based on results from research question 3, serial X-ray exposure does not cause or exacerbate dysphagia. However, we observed fur depigmentation and dry eyes on the side of the body that was closest to the X-ray source (i.e., the right side), as shown in **Figure 6**. This observation is indicative of surface level radiation toxicity from our VFSS system. Although we did not keep detailed records for this adverse outcome, it was readily apparent in the majority of mice, with the exception of white mice which are already depigmented.



Figure 6. Radiation Toxicity. Mice with serial VFSS testing developed signs of surface-level radiation toxicity affecting the skin and eyes. Depigmentation of the fur and excessive drying of the eyes has been observed on the side of the body closest to the X-ray source, indicative of surface absorption of low energy X-ray scatter from our VFSS system.

Based on our finding that serial X-ray exposure did not influence dysphagia severity, we combined data from the serial and single X-ray exposure groups at disease end-stage. This approach markedly increased our sample size, thereby allowing for additional statistical analyses to investigate differences in dysphagia relative to disease phenotypes. For this purpose, we classified mice into two phenotype groups: 1) predominantly hindlimb paralysis (n=11), or 2) combination of forelimb and hindlimb paralysis (n=14). Independent samples T-tests (2-sided) revealed statistically significant differences between phenotypes for 3 of the 8 VFSS metrics, as shown in **Table 6**.

Table 6. MEAN DIFFERENCE, STANDARD ERROR DIFFERENCE, AND P VALUE FOR VFSS METRICS AT DISEASE END-STAGE FOR COMPARISON OF HINDLIMB (n=11) AND FORELIMB + HINDLIMB PARALYSIS (n= 14)

Swallow Metrics	Mean Difference	Std. Error Difference	p value
Lick Rate	.016	.188	.931
Swallow Rate	.399	.167	.019
Lick-Swallow Ratio	-.941	.378	.015
Inter-Swallow interval	-.211	.067	.002
Pharyngeal Transit Time	.004	.003	.177
Esophageal Transit Time	.149	.098	.134
Effective Esophageal Swallows	.000	.118	1.000
Swallows to Clear Esophagus	.222	.186	.236

Interestingly, lick rate was not statistically different between the two ALS phenotypes, although it was significantly slower for both phenotypes when compared to control mice. Thus, lick rate impairment is a general indicator of dysphagia in this mouse model of ALS, regardless of phenotype. In contrast, mice with forelimb+hindlimb paralysis had more severely impaired swallow rates compared to mice with only hindlimb paralysis, although both groups had significantly slower swallow rates compared to controls. Similarly, mice with forelimb+hindlimb paralysis had significantly longer inter-swallow interval durations compared to mice with hindlimb paralysis only, although both groups had significantly longer inter-swallow interval durations compared to controls. Perhaps most fascinating was the finding that lick-swallow ratio did not differ between hindlimb phenotype and control mice, although it was significantly longer (approximately 1 additional lick per swallow) for mice with forelimb+hindlimb paralysis. Thus, forelimb affected *LCN-SOD1* mice have more impaired swallow function than *LCN-SOD1* mice with only hindlimb paralysis. These results are illustrated in **Figure 7**.

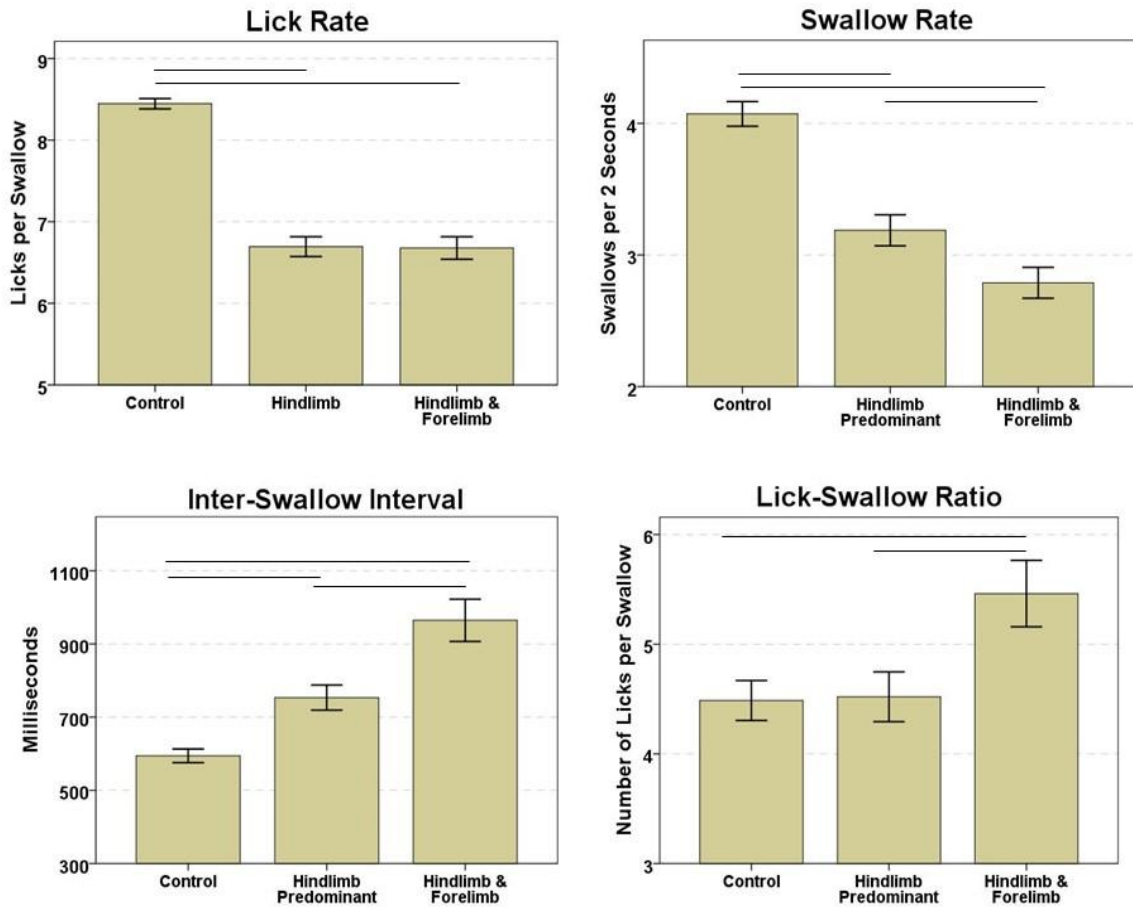


Figure 7. Dysphagia severity differences at end-stage between phenotypes. Lick rate was not significantly different between phenotypes. Inter-swallow interval and swallow rate were more severely impaired for hindlimb and forelimb mice, than for hindlimb predominant mice, and both phenotypes were significantly different compared to controls. Compared to controls, lick swallow ratio was significantly different for the hindlimb and forelimb phenotype, but not the hindlimb predominant phenotype. Lines denote statistical significance ($p < .05$) between groups; Error bars = mean \pm 1 standard error of the mean (SEM).

CHAPTER IV: DISCUSSION

The primary goal of this project was to establish the timing of dysphagia onset and rate of progression in a mouse model of ALS using our established VFSS protocol to quantify 8 swallow metrics. A secondary goal was to determine if serial (i.e., monthly) radiation exposure during VFSS testing over the lifespan would result in more severe dysphagia. To achieve these goals, we tested two cohorts of mice from our *LCN-SOD1* colony: a single X-ray exposure group and a serial X-ray exposure group, each containing transgenic and control mice. The single X-ray exposure group was tested once at disease endstage. The serial X-ray exposure group was tested monthly across the lifespan, starting at two months of age until disease end-stage, resulting in 6 to 9 radiation exposures per mouse. Our purpose for investigating these goals was twofold: 1) to determine a therapeutic window for future dysphagia treatment investigations with this mouse model of ALS, and 2) to determine if dysphagia severity is worsened by serial x-ray exposure, which would confound our study outcomes.

We know from a prior thesis project in our lab that *LCN-SOD1* mice do indeed develop dysphagia at disease end-stage (Robbins et al., 2015). For the current study, we have reproduced this finding by showing that *LCN-SOD1* mice at disease end-stage have significantly impaired lick rate, swallow rate, inter-swallow-interval, effective esophageal swallows, and number of swallows to clear esophagus. However, a novel finding is that dysphagia onset in *LCN-SOD1* mice emerges after six months of age, while mice are rapidly progressing through

disease stages. This finding was surprising because our lab has previously shown that in the high copy number *SOD1* (*HCN-SOD1*) mouse model of ALS, dysphagia emerges by 21 days of age while mice are still maturing (Daghlis, 2015). Thus, compared to the *HCN-SOD1* model, dysphagia onset is markedly delayed in *LCN-SOD1* mice. As a result, *LCN-SOD1* mice are better-suited (compared to *HCN-SOD1* mice) for translational dysphagia treatment investigations because there is a long pre-clinical stage in which mice are asymptomatic, similar to human ALS.

Another novel finding of this study was that serial X-ray exposure across the lifespan (starting at 2 months of age until disease end-stage) in *LCN-SOD1* mice did *not* alter dysphagia severity, when compared to VFSS data from the single X-ray exposure group. In other words, swallowing function was equally impaired in both groups of *LCN-SOD1* mice at disease end-stage, regardless of the number of X-ray exposures. Our initial interpretation of this finding was that serial VFSS would *not* be necessary for our future research, given our previously discussed finding that swallow metrics do not become impaired until after 6 months of age. That is to say, serial VFSS would not be needed prior to 6 months of age, as swallow function remains normal during that time.

Further support for this plan was our finding that the majority of mice *did* develop evidence of surface-level radiation toxicity (fur depigmentation and dry eyes) as the number of X-ray exposures increased, even though it did not affect swallow function. Therefore, proactive measures are certainly warranted to reduce radiation exposure and thereby prevent skin and eye morbidities for our

longitudinal dysphagia investigations. However, our lab's ongoing collaboration with computer scientists at MU have resulted in a prototype jaw tracking algorithm that can perform automated quantification of swallow measures from VFSS videos of mice.

Therefore, VFSS will remain essential to hasten our lab's research productivity as we progress toward larger studies. Additionally, a calibration marker on our VFSS machine will permit distance measurements (e.g., jaw opening distance for each jaw cycle) and tracking of rhythm, adding to the rationale for continuing use of VFSS. We expect these measures may be more sensitive to change over time. Furthermore, automation will calculate lick rate as a fraction, rather than a whole number, which may unmask larger differences in lick rate between groups. Moreover, using automation for mastication rate as a quantifiable swallow metric may provide an additional behavioral biomarker to identify dysphagia onset and track dysphagia progression over time. Our lab has previously shown that mastication rate is impaired early in *HCN-SOD1* mice, shortly after lick rate deficit emerges. However, this metric has not yet been investigated in *LCN-SOD1* mice.

Yet another novelty of our study is that we were able to determine differences in dysphagia severity at disease end-stage relative to disease phenotype. Compared to controls, both phenotypes (hindlimb paralysis, hindlimb + forelimb paralysis) were significantly different for two swallow metrics (swallow rate and inter-swallow interval), though mice with hindlimb + forelimb paralysis

were more severely impaired than mice with hindlimb paralysis only for both swallow rate and inter-swallow interval. Compared to controls, lick-swallow ratio was significantly longer for the hindlimb + forelimb phenotype, but not the hindlimb only phenotype. Throughout our investigations with the *LCN-SOD1* mouse model, additional phenotypic presentations have become apparent. We hope that as we are better able to characterize these phenotypes, we will be able to better detect differences in the timing of dysphagia onset and rate of progression, which will provide important information for future treatment investigations.

An unexpected finding from this study was that *LCN-SOD1* mice had significantly more effective esophageal swallows and required significantly fewer number of swallows to clear the esophagus at disease end-stage. Initially, this finding was counter intuitive, as we interpreted these behaviors as improvements rather than deficits in esophageal function. However, our observations of control mice provide insight to explain this finding. The significantly fast lick and swallow rates of control mice result in convergence of multiple successive boluses in the esophagus. In contrast, we suspect the slower lick and swallow rates of *LCN-SOD1* mice result in passage of single boluses through the esophagus, which was our operational definition of “effective esophageal swallows.” We suspect this behavior may still be problematic because the slower rate of drinking in *LCN-SOD1* mice may result in reduced liquid intake that compromises nutritional status. Thus, objective measures of nutritional status (e.g., liquid volume per unit of time) may be important to include in our future studies.

Limitations

While this study provided valuable information on the timing of dysphagia onset in *LCN-SOD1* mice and the effect of serial radiation in this mouse model, there are several limitations that warrant consideration and further investigation. A primary limitation was the small sample size of the serial X-ray exposure group, which was further compounded by the rapid attrition rate of mice as they rapidly progressed to disease end-stage. As a result, we were not able to closely characterize the onset and progression of dysphagia in this mouse model. Our lab is currently using VFSS to test a second cohort of mice using the serial exposure method outlined in this thesis project, which we hope will aid in the characterization of dysphagia onset and progression in this *LCN-SOD1* mouse model.

Another limitation of this project was that our current VFSS technology captures videos at 30 fps, which is too slow to permit visualization and quantification of the pharyngeal stage of swallowing beyond swallow rate. For example, pharyngeal transit time in mice typically takes only 2-3 frames to complete because the structures in the pharynx and larynx are moving approximately 10 times faster than people (Lever, Braun, et al., 2015). As a result, we were unable to visualize all of the pharyngeal swallow events that are readily apparent in VFSS with people when recorded at the 30 fps, such as laryngeal excursion, epiglottic inversion, and pharyngeal contraction. We hypothesize that video recordings at a higher frame rate (100 fps or more) may reveal significant findings with regard to pharyngeal transit time in this tiny animal model.

Esophageal transit time also posed a problem because the stomach is partially full in most mice before video recording of the esophageal stage of swallowing takes place. Our standard protocol entails focusing on the oral and pharyngeal stages of swallowing (i.e., Position 1) first, and then moving to the esophageal stage of swallowing (i.e., Position 2). We have found this approach results in variable filling of the stomach by the time Position 2 is captured, which obscures the distal segment of the esophagus where it enters the stomach. Therefore, we have used the fundus of the stomach as the anatomical landmark that the bolus tail must pass through when determining the end of the esophageal stage of swallowing. We are currently conducting a pilot study to determine if reversing the order of video capture (i.e., Position 2 first, followed by Position 1) will enable detection of longer esophageal transit times in our *LCN-SOD1* mice compared to controls, thus providing another robust measure of dysphagia for our future studies.

Unfortunately, bolus area calculations were inaccurate due to an alteration of the calibration marker in the field of view during VFSS. Although this error can be overcome by retracing all of the bolus areas for every mouse to recalculate bolus area, which was our intention, it is an extremely labor intensive process that could not be completed within the time frame of this thesis project. Moving forward, modification of our operational definition of bolus area is underway to assure the jaw is aligned bilaterally (i.e., the jaw should appear as a single bone) for all bolus area measurements to improve accuracy of this swallow metric.

Future directions

Now that we have established the *LCN-SOD1* mouse model of ALS has a delayed onset (i.e., adult onset) of dysphagia, we are ready to begin pre-clinical treatment investigations to ultimately benefit people with ALS. Examples of interest to our lab include tongue resistance exercise, electrical stimulation of the laryngeal nerves, serotonin supplementation, and menthol ingestion. The next objective is to determine which of these treatments can preserve swallow function, and hence increase survival, in *LCN-SOD1* mice.

The results of this study demonstrate that for our future studies with *LCN-SOD1* mice, serial VFSS may not be necessary until mice reach 6 months of age. However, we will reserve this decision pending data analysis of the final cohort of mice undergoing serial radiation exposure, which are just now reaching disease end-stage. Additionally, expanding our VFSS protocol to include food items, rather than only thin liquid, would provide new swallow metrics to investigate, which may facilitate earlier detection and better tracking of dysphagia in this mouse model. Moreover, our lab is collaborating with computer scientists at MU to develop software for semi-automated analysis of our VFSS videos, which will hopefully result in more accurate and efficient data analysis and greater sensitivity of swallow metrics (e.g., lick rate measured as fractions rather than whole numbers). Finally, although we have shown that serial radiation exposure does not cause dysphagia, our lab is currently undergoing modifications to our VFSS system. For example, our lab is currently collaborating with engineering students to create a

motion-activated system that turns on the X-ray beam only when the mouse approaches the drinking bowl. We are also designing low-energy filters to prevent the mice from absorbing the low-energy scatter that is emitted during testing. We are confident that our greater understanding of dysphagia onset and progression in this mouse model, along with the effects of serial X-ray, will allow us to move forward with an improved protocol in pursuit of finding effective treatments for dysphagia in ALS.

References

- Acevedo-Arozena, A., Kalmar, B., Essa, S., Ricketts, T., Joyce, P., Kent, R., Fisher, E. M. (2011). A comprehensive assessment of the SOD1G93A low-copy transgenic mouse, which models human amyotrophic lateral sclerosis. *Dis Model Mech*, 4(5), 686-700.
- Alexander, G. M., Erwin, K. L., Byers, N., Deitch, J. S., Augelli, B. J., Blankenhorn, E. P., & Heiman-Patterson, T. D. (2004). Effect of transgene copy number on survival in the G93A SOD1 transgenic mouse model of ALS. *Brain Res Mol Brain Res*, 130(1-2), 7-15.
- Association, A. (2015). Epidemiology of ALS and Suspected Clusters. Retrieved from <http://www.alsa.org/als-care/resources/publications-videos/factsheets/epidemiology.html>
- Association, A. (2016). Who gets ALS? Retrieved from <http://www.alsa.org/about-als/who-gets-als.html>
- Association, M. D. (2015). Amyotrophic Lateral Sclerosis.
- Belsh, J. M. (1996). Clinical presentation and course of ALS. *Amyotrophic lateral sclerosis: diagnosis and management*. Armonk, NY: Futura Publishing, 47-83.
- Boillee, S., Vande Velde, C., & Cleveland, D. W. (2006). ALS: a disease of motor neurons and their nonneuronal neighbors. *Neuron*, 52(1), 39-59.
- Braun, S. (2015). *Videofluoroscopic characterization of dysphagia in the low copy number SOD1-G93A transgenic mouse model of ALS*. (Master of Health Science), University of Missouri, University of Missouri.
- Brooks, B. R., Miller, R. G., Swash, M., Munsat, T. L., & Diseases, W. F. o. N. R. G. o. M. N. (2000). El Escorial revisited: revised criteria for the diagnosis of amyotrophic lateral sclerosis. *Amyotroph Lateral Scler Other Motor Neuron Disord*, 1(5), 293-299.
- Brooks, B. R., & Sanjak, M. (2004). Disease-modifying drug therapies. *Amyotroph Lateral Scler Other Motor Neuron Disord*, 5 Suppl 1, 68-75.
- Brujin, L. I., Miller, T. M., & Cleveland, D. W. (2004). Unraveling the mechanisms involved in motor neuron degeneration in ALS. *Annu Rev Neurosci*, 27, 723-749.

- Chen, S., Sayana, P., Zhang, X., & Le, W. (2013). Genetics of amyotrophic lateral sclerosis: an update. *Mol Neurodegener*, 8(1), 28.
- Christensen, P. B., Hojer-Pedersen, E., & Jensen, N. B. (1990). Survival of patients with amyotrophic lateral sclerosis in 2 Danish counties. *Neurology*, 40(4), 600-604.
- Cleveland, D. W., & Rothstein, J. D. (2001). From Charcot to Lou Gehrig: deciphering selective motor neuron death in ALS. *Nat Rev Neurosci*, 2(11), 806-819.
- Corcia, P., Pradat, P. F., Salachas, F., Bruneteau, G., Forestier, N., Seilhean, D., Meininger, V. (2008). Causes of death in a post-mortem series of ALS patients. *Amyotroph Lateral Scler*, 9(1), 59-62.
- Daghlas, I., Martin, H., Kadosh, M., Goding, G., Mancini, S., Dougherty, D., Harris, K., Robbins, K., Lever, T. (2015). Effect of gene copy number on dysphagia onset in SOD1-G93A transgenic mice. *Amyotrophic Lateral Sclerosis and Frontotemporal Degeneration*, 16(1), 217-226.
- Dal Bello-Haas, V., & Florence, J. (2013). *Therapeutic exercise for people with amyotrophic lateral sclerosis or motor neuron disease (Review)*. The Cochrane Library 2013, Issue 5, John Wiley & Sons, Ltd.
- Dal Canto, M. C., & Gurney, M. E. (1997). A low expressor line of transgenic mice carrying a mutant human Cu,Zn superoxide dismutase (SOD1) gene develops pathological changes that most closely resemble those in human amyotrophic lateral sclerosis. *Acta Neuropathol*, 93(6), 537-550.
- DePaul, R., Abbs, J. H., Caligiuri, M., Gracco, V. L., & Brooks, B. R. (1988). Hypoglossal, trigeminal, and facial motoneuron involvement in amyotrophic lateral sclerosis. *Neurology*, 38(2), 281-283.
- DePaul, R., & Brooks, B. R. (1993). Multiple orofacial indices in amyotrophic lateral sclerosis. *J Speech Hear Res*, 36(6), 1158-1167.
- Dworkin, J. P. (1980). Tongue strength measurement in patients with amyotrophic lateral sclerosis: qualitative vs quantitative procedures. *Arch Phys Med Rehabil*, 61(9), 422-424.
- Ertekin, C., Aydogdu, I., Yuceyar, N., Kiylioglu, N., Tarlaci, S., & Uludag, B. (2000). Pathophysiological mechanisms of oropharyngeal dysphagia in amyotrophic lateral sclerosis. *Brain*, 123 (Pt 1), 125-140.

- Gonzalez de Aguilar, J. L., Echaniz-Laguna, A., Fergani, A., Rene, F., Meininger, V., Loeffler, J. P., & Dupuis, L. (2007). Amyotrophic lateral sclerosis: all roads lead to Rome. *J Neurochem*, *101*(5), 1153-1160.
- Gurney, M., Pu, H., Chiu, A., Dal Canto, M., Polchow, C., Alexander, D., Deng, H. (1994). Motor neuron degeneration in mice that express a human Cu,Zn superoxide dismutase mutation. *Science*, *264*, 1772-1775.
- Gurney, M. E. (1997). The use of transgenic mouse models of amyotrophic lateral sclerosis in preclinical drug studies. *J Neurol Sci*, *152 Suppl 1*, S67-73.
- Gwinn, K., Corriveau, R. A., Mitsumoto, H., Bednarz, K., Brown, R. H., Cudkovicz, M., Group, A. R. (2007). Amyotrophic lateral sclerosis: an emerging era of collaborative gene discovery. *PLoS One*, *2*(12), e1254.
- Hadjikoutis, S., & Wiles, C. M. (2001). Respiratory complications related to bulbar dysfunction in motor neuron disease. *Acta Neurol Scand*, *103*(4), 207-213.
- Hayworth, C. R., & Gonzalez-Lima, F. (2009). Pre-symptomatic detection of chronic motor deficits and genotype prediction in congenic b6.sod1g93a als mouse model. *Neuroscience*, *164*(3), 975-985.
- Higo, R., Tayama, N., & Nito, T. (2004). Longitudinal analysis of progression of dysphagia in amyotrophic lateral sclerosis. *Auris Nasus Larynx*, *31*(3), 247-254.
- Higo, R., Tayama, N., Watanabe, T., & Nitou, T. (2002). Videomanofluorometric study in amyotrophic lateral sclerosis. *Laryngoscope*, *112*(5), 911-917.
- Hillel, A. D., & Miller, R. (1989). Bulbar amyotrophic lateral sclerosis: patterns of progression and clinical management. *Head Neck*, *11*(1), 51-59.
- Hillel, A. D., & Miller, R. M. (1987). Management of bulbar symptoms in amyotrophic lateral sclerosis. *Adv Exp Med Biol*, *209*, 201-221.
- Institute, A. T. D. (2015). ALS Frequently Asked Questions. Retrieved from <http://www.alstdi.org/about-als-tdi/als-faq/>
- Jaarsma, D., Teuling, E., Haasdijk, E., De Zeeuw, C., & Hoogenraad, C. (2008). Neuron-specific expression of mutant superoxide dismutase is sufficient to induce amyotrophic lateral sclerosis in transgenic mice. *The Journal of Neuroscience*, *28*(9), 2075-2088.

- Kawai, S., Tsukuda, M., Mochimatsu, I., Enomoto, H., Kagesato, Y., Hirose, H., Suzuki, Y. (2003). A study of the early stage of Dysphagia in amyotrophic lateral sclerosis. *Dysphagia*, 18(1), 1-8.
- Kiernan, M. C., Vucic, S., Cheah, B. C., Turner, M. R., Eisen, A., Hardiman, O., Zoing, M. C. (2011). Amyotrophic lateral sclerosis. *Lancet*, 377(9769), 942-955.
- Kuhnlein, P., Gdynia, H. J., Sperfeld, A. D., Lindner-Pfleghar, B., Ludolph, A. C., Prosiegel, M., & Riecker, A. (2008). Diagnosis and treatment of bulbar symptoms in amyotrophic lateral sclerosis. *Nat Clin Pract Neurol*, 4(7), 366-374.
- Kunst, C. B. (2004). Complex genetics of amyotrophic lateral sclerosis. *Am J Hum Genet*, 75(6), 933-947.
- Lacomblez, L., Bensimon, G., Leigh, P. N., Guillet, P., Powe, L., Durrleman, S., Meininger, V. (1996). A confirmatory dose-ranging study of riluzole in ALS. ALS/Riluzole Study Group-II. *Neurology*, 47(6 Suppl 4), S242-250.
- Leder, S. B., Novella, S., & Patwa, H. (2004). Use of fiberoptic endoscopic evaluation of swallowing (FEES) in patients with amyotrophic lateral sclerosis. *Dysphagia*, 19(3), 177-181.
- Lever, T. E., Braun, S. M., Brooks, R. T., Harris, R. A., Littrell, L. L., Neff, R. M., Ulsas, M. A. (2015). Adapting human videofluoroscopic swallow study methods to detect and characterize dysphagia in murine disease models. *Journal of visualized experiments: JoVE*, (97).
- Lever, T. E., Brooks, R. T., Thombs, L. A., Littrell, L. L., Harris, R. A., Allen, M. J., Robbins, K. L. (2015). Videofluoroscopic Validation of a Translational Murine Model of Presbyphagia. *Dysphagia*.
- Lever, T. E., Gorsek, A., Cox, K. T., O'Brien, K. F., Capra, N. F., Hough, M. S., & Murashov, A. K. (2009). An animal model of oral dysphagia in amyotrophic lateral sclerosis. *Dysphagia*, 24(2), 180-195.
- Lever, T. E., Simon, E., Cox, K. T., Capra, N. F., O'Brien, K. F., Hough, M. S., & Murashov, A. K. (2010). A mouse model of pharyngeal dysphagia in amyotrophic lateral sclerosis. *Dysphagia*, 25(2), 112-126.
- Logemann, J. A. (2006). Medical and Rehabilitative Therapy of Oral, Pharyngeal Motor Disorders, *GI Motility Online*, 2006.

- Mead, R. J., Bennett, E. J., Kennerley, A. J., Sharp, P., Sunyach, C., Kasher, P., Shaw, P. J. (2011). Optimised and rapid pre-clinical screening in the SOD1(G93A) transgenic mouse model of amyotrophic lateral sclerosis (ALS). *PLoS One*, 6(8), e23244.
- Milanese, M., Giribaldi, F., Melone, M., Bonifacino, T., Musante, I., Carminati, E., Bonanno, G. (2014). Knocking down metabotropic glutamate receptor 1 improves survival and disease progression in the SOD1(G93A) mouse model of amyotrophic lateral sclerosis. *Neurobiol Dis*, 64, 48-59.
- Miller, R. G., Mitchell, J. D., Lyon, M., & Moore, D. H. (2007). Riluzole for amyotrophic lateral sclerosis (ALS)/motor neuron disease (MND). *The Cochrane Library*.
- Miller, R. G., Mitchell, J. D., & Moore, D. H. (2012). Riluzole for amyotrophic lateral sclerosis (ALS)/motor neuron disease (MND). *The Cochrane Library*.
- Mitchell, J. D., & Borasio, G. D. (2007). Amyotrophic lateral sclerosis. *Lancet*, 369(9578), 2031-2041.
- Mitsumoto, H., Davidson, M., Moore, D., Gad, N., Brandis, M., Ringel, S., Anderson, F. A. (2003). Percutaneous endoscopic gastrostomy (PEG) in patients with ALS and bulbar dysfunction. *Amyotroph Lateral Scler Other Motor Neuron Disord*, 4(3), 177-185.
- Nelson, L. M. (1995). Epidemiology of ALS. *Clin Neurosci*, 3(6), 327-331.
- Neurobiology Research and the Laboratory Mouse: A Jackson Laboratory Resource Manual*. (2008). Bar Harbor, ME: The Jackson Laboratory.
- Oliver, D. (1996). The quality of care and symptom control--the effects on the terminal phase of ALS/MND. *J Neurol Sci*, 139 Suppl, 134-136.
- Orsini, M., Oliveira, A. B., Nascimento, O. J., Reis, C. H., Leite, M. A., de Souza, J. A., Smidt, B. (2015). Amyotrophic Lateral Sclerosis: New Perspectives and Update. *Neurol Int*, 7(2), 5885.
- Pfohl, S. R., Halicek, M. T., & Mitchell, C. S. (2015). Characterization of the Contribution of Genetic Background and Gender to Disease Progression in the SOD1 G93A Mouse Model of Amyotrophic Lateral Sclerosis: A Meta-Analysis. *J Neuromuscul Dis*, 2(2), 137-150.
- Plowman, E. K. (2015). Is There a Role for Exercise in the Management of Bulbar Dysfunction in Amyotrophic Lateral Sclerosis? *J Speech Lang Hear Res*, 58(4), 1151-1166.

- Preston, D. C., Shapiro, B.E. (2005). Amyotrophic Lateral Sclerosis and its Variants. In *Electromyography and Neuromuscular Disorders: Clinical-Electrophysiological Correlations*. (2 ed., pp. 423-437). Philadelphia: Elsevier.
- Rao, M. V., Campbell, J., Palaniappan, A., Kumar, A., & Nixon, R. A. (2016). Calpastatin inhibits motor neuron death and increases survival of hSOD1(G93A) mice. *J Neurochem*, 137(2), 253-265.
- Ravits, J., Appel, S., Baloh, R. H., Barohn, R., Brooks, B. R., Elman, L., Ringel, S. (2013). Deciphering amyotrophic lateral sclerosis: what phenotype, neuropathology and genetics are telling us about pathogenesis. *Amyotroph Lateral Scler Frontotemporal Degener*, 14 Suppl 1, 5-18.
- Rio, A., Ellis, C., Shaw, C., Willey, E., Ampong, M. A., Wijesekera, L., Al-Chalabi, A. (2010). Nutritional factors associated with survival following enteral tube feeding in patients with motor neurone disease. *J Hum Nutr Diet*, 23(4), 408-415.
- Robbins, K., Allen, M., & Lever, T. (2015). Low copy number SOD1-G93A mice are better suited for dysphagia research compared to the high copy number model. *Amyotrophic Lateral Sclerosis and Frontotemporal Degeneration*, 16, 217-226.
- Rosen, D. R. (1993). Mutations in Cu/Zn superoxide dismutase gene are associated with familial amyotrophic lateral sclerosis. *Nature*, 364(6435), 362.
- Rosen, D. R., Siddique, T., Patterson, D., Figlewicz, D. A., Sapp, P., Hentati, A., Gaston, S.M. (1993). Mutations in Cu/Zn superoxide dismutase gene are associated with familial amyotrophic lateral sclerosis. *Nature*, 362(6415), 59-62.
- Ryuzabaro, H., Niro, T., & Takaharu, N. (2004). Longitudinal analysis of progression of dysphagia in amyotrophic lateral sclerosis. *Auris Nasus Larynx*, 31, 247-254.
- Sejvar, J. J., Holman, R. C., Bresee, J. S., Kochanek, K. D., & Schonberger, L. B. (2005). Amyotrophic lateral sclerosis mortality in the United States, 1979-2001. *Neuroepidemiology*, 25(3), 144-152.
- Shigemitsu, H., & Afshar, K. (2007). Aspiration pneumonias: under-diagnosed and under-treated. *Curr Opin Pulm Med*, 13(3), 192-198.

- Smittkamp, S. E., Brown, J. W., & Stanford, J. A. (2008). Time-course and characterization of orolingual motor deficits in B6SJL-Tg(SOD1-G93A)1Gur/J mice. *Neuroscience*, *151*(2), 613-621.
- Spataro, R., Lo Re, M., Piccoli, T., Piccoli, F., & La Bella, V. (2010). Causes and place of death in Italian patients with amyotrophic lateral sclerosis. *Acta Neurol Scand*, *122*(3), 217-223.
- Stoica, L., Todeasa, S. H., Cabrera, G. T., Salameh, J. S., ElMallah, M. K., Mueller, C., Sena-Esteves, M. (2016). Adeno-associated virus-delivered artificial microRNA extends survival and delays paralysis in an amyotrophic lateral sclerosis mouse model. *Ann Neurol*, *79*(4), 687-700.
- Su, X. W., Nandar, W., Neely, E. B., Simmons, Z., & Connor, J. R. (2016). Statins accelerate disease progression and shorten survival in SOD1(G93A) mice. *Muscle Nerve*, *54*(2), 284-291.
- Tayama, N. (1995). [Dysphagia in amyotrophic lateral sclerosis--the mechanism and managements]. *Rinsho Shinkeigaku*, *35*(12), 1557-1559.
- Ticozzi, N., Tiloca, C., Morelli, C., Colombrita, C., Poletti, B., Doretto, A., Silani, V. (2011). Genetics of familial Amyotrophic lateral sclerosis. *Arch Ital Biol*, *149*(1), 65-82.
- Turner, M. R., Hardiman, O., Benatar, M., Brooks, B. R., Chio, A., de Carvalho, M., Kiernan, M. C. (2013). Controversies and priorities in amyotrophic lateral sclerosis. *Lancet Neurol*, *12*(3), 310-322.
- Wang, Y., Duan, W., Wang, W., Wen, D., Liu, Y., Li, Z., Li, C. (2016). scAAV9-VEGF prolongs the survival of transgenic ALS mice by promoting activation of M2 microglia and the PI3K/Akt pathway. *Brain Research*, *1648*, 1-10.
- Weikamp, J. G., Schelhaas, H. J., Hendriks, J. C., de Swart, B. J., & Geurts, A. C. (2012). Prognostic value of decreased tongue strength on survival time in patients with amyotrophic lateral sclerosis. *J Neurol*, *259*(11), 2360-2365.
- Wijesekera, L. C., & Leigh, P. N. (2009). Amyotrophic lateral sclerosis. *Orphanet Journal of Rare Diseases*, *4*(1), 3.
- Wright, R., & Jordan, C. (1997). Videofluoroscopic evaluation of dysphagia in motor neurone disease with modified barium swallow. *Palliat Med*, *11*(1), 44-48.

Yoshida, S., Mulder, D. W., Kurland, L. T., Chu, C. P., & Okazaki, H. (1986). Follow-up study on amyotrophic lateral sclerosis in Rochester, Minn., 1925 through 1984. *Neuroepidemiology*, 5(2), 61-70.